RESEARCH ARTICLE

Influence of thermo-oxidative aging on the mechanical properties of the bead foams made of polycarbonate and polypropylene

Nick Weingart[1] | Daniel Raps[2] | Marc Lamka[1] | Martin Demleitner[1] |
Volker Altstädt[1] | Holger Ruckdäschel[1]

[1]Department of Polymer Engineering, University of Bayreuth, Bayreuth, Germany

[2]Physics & Material Science EMEA, Covestro Deutschland AG, Leverkusen, Germany

Correspondence
Holger Ruckdäschel, Department of Polymer Engineering, University of Bayreuth, Bayreuth, Germany.
Email: holger.ruckdaeschel@uni-bayreuth.de

Abstract

Bead foams made from standard polymers such as expanded polystyrene (EPS) or expanded polypropylene (EPP) are widely used in everyday products. In order to expand the application window of bead foams, the industry, such as the automotive industry among others, is striving for higher-performance materials to create a lightweight material for high-temperature applications. New bead foams such as expanded polycarbonate (EPC) are emerging to offer a wider range of solutions, with thermo-mechanical properties constantly improving. EPC has excellent mechanical properties, which has been shown in our previous work. To fully understand the capabilities of a material for high-temperature applications, it is important to know what happens when it is exposed to conditions, that lead to aging. Morphological studies, as well as mechanical characterizations help to determine the properties of EPC compared to EPP. Since thermo-oxidative aging of thermoplastic foams is almost unexplored, especially in the field of bead foams, this research represents an important contribution to the understanding of material behavior and development. Time-consuming aging tests were able to confirm that EPC is not only a very thermally stable material, but also able to provide reasonable mechanical performance after aging, compared to EPP.

KEYWORDS

aging, bead foam, EPC, EPP, expanded polycarbonate, mechanics

1 | INTRODUCTION

In the last 50 years, polymers have become part of our daily lives. Most of the circulating plastics are based on standard commodity polymers as products are designed for a specific application. One of these criteria is the service temperature, as the use of polymers is usually limited by an upper and lower temperature specific to each plastic. These limits correspond to the application temperature range of the polymers and are mainly determined by two factors. On the one hand, short-term temperature affects such as reversible softening or embrittlement and, on the other hand, the behavior under long-term temperature exposure with or without

additional load. Long-term temperature effects cannot be extrapolated with short-term ones, since in this case aging and relaxation processes are also involved.[1] During processing and application, polymers are exposed to particular thermal and oxidative stress. During processing in the absence of oxygen in the molten state, plastics are briefly exposed to high temperatures and additional shearing. With normal use under environmental influences, the plastic is exposed to oxidative influences, but at rather low temperatures. From this can be concluded that, in addition to the temperature, the oxygen in the environment also has a strong influence on the aging of plastics.[2]

The effect of UV radiation must also be taken into account. Material-intrinsic factors such as component thickness or chemical structure as well as external factors depending on the environmental conditions influence the extent and type of aging and thus the speed of the associated degradation. Mechanical, electrical and thermal properties, as well as crystallinity, color (yellowing), surface structure (cracks) or chemical resistance are among the most significant aging phenomena. Considering the time-dependent, irreversible aging, materials may not only deteriorate, but also improve.[2] In general, aging factors are distinguished between internal and external origin. Internal aging factors are due to thermodynamically unstable conditions in the material. These include, for example, internal stresses, limited mixing or insufficient compatibility of the components. External aging factors are chemical or physical environmental influences that affect the material, for example B. mechanical loads or temperature effects. Accordingly, thermo-oxidative aging belongs to the external aging factors.[3] More specifically, as the effect of oxygen occurs simultaneously with thermal aging, additional reactions are initiated and oxygen is incorporated into molecular chains. Chemical processes thus lead to undesirable degradation reactions (e.g. chain scission) in macromolecules due to thermo-oxidative aging.[2,3] Taking radical formation as an example, it is shown that peroxide radicals are formed with the addition of oxygen (Equation 1). The reason for this is sufficient energy in the form of heat and the resulting homolytic bond cleavage in the macromolecular chains (R-H). Peroxide radicals can therefore remain as hydroperoxides (Equation 1,2).[2,3]

$$R^* + O_2 \rightarrow ROO^*. \tag{1}$$

$$ROO^* + R-H \rightarrow ROOH + R^*. \tag{2}$$
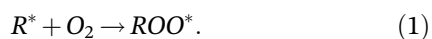
In addition, physical degradation processes can also occur during thermo-oxidative aging. These include postcrystallization, T_g depression, degradation of residual stresses or orientations, loss of plasticizers or agglomeration. Long-term behavior and service life from time-lapse tests (artificial aging) or short-term tests must be viewed critically, because complex aging processes occur.

As mentioned earlier, there is some literature available on thermo-oxidative aging of PC and PP, but almost none for thermoplastic foams. Usual applications where expanded polypropylene (EPP) is subjected to thermal aging are either insulation or packaging as thermo-boxes or the usage as core material for sun-visors in automotive. Due to a higher glass transition temperature, expanded polycarbonate (EPC) is designated for near-engine applications or battery covers, where it would be subjected to a cyclic temperature load. The most interesting work on polycarbonate and polypropylene can be found in Table 1. Most of the available work in the field of physical aging relates to annealing and not explicitly to thermo-oxidative aging.

Law et al. and Steiner et al. discussed the thermal aging of isotactic polypropylene 20 years ago. Law et al. could not determine any change in the crystalline phases. However, a reduction of the amorphous regions after aging at 90 and 140 °C was reported, while no traces on vinyl groups could be detected by FTIR measurements.[12] Steiner et al. concluded that i-PP lost performance in elongation at break and tensile stress due to aging, while the dielectric loss factor increased and resulted in a loss of thermo-oxidative stability.[9] Schwarz et al. and Rjeb et al. also dealt with polypropylene and its aging. Regarding tensile properties, Schwarz et al. observed an increase in tensile modulus and a shift in yield strength toward higher stresses and lower strains.[10] Thermal degradation as a function of time was detected by Rjeb et al. using DSC and TG measurements.[11] Last but not least, Mourad et al. dealt with modified PP blends. Here, no changes in behavior under tensile stress or hardness could be detected. In addition, the thermal stability remained unchanged after aging.[13]

In the case of polycarbonate, Bertilsson et al.[4] also examined PC/PBT blends. They described a loss of ductility during aging, possibly due to densification of the amorphous phases. In addition, Suzuki et al.[7] investigated the thermal aging resistance of polycarbonate blends. He aged a low MW-PC of 19,000 g/mol for up to 48 h at 120 °C and characterized the materials. He determined in tensile tests, that aging of PC leads to a hardening and thus embrittlement of the material. The yield strength increased by 25% while the modulus dropped slightly. In his research, the embrittlement could be prevented by the addition of SEBS. In another study,[5] impact modified polycarbonate showed no change during thermal aging because the modifier was not thermally stable enough. Further, Dhara et al.[6] dealt with a polycarbonate

TABLE 1 Literature review for neat thermal-oxidative aged polycarbonate and polypropylene.

Author	Polymer	Aging	Investigations
Guerdoux et al. (1981)	PC and PMMA	Temp.: 30 °C Time: 24 h	Depolarization, dielectric properties
Washer (1984)	PC	Temp.: 111, 119, 130 °C Time: 2–256 h	Density, DSC
Haidar et al. (1989)	PC	Temp.: 120 °C Time: up to 720 h	Tensile
Bartos et al. (1989)	PC	Temp.: 60, 125 °C Time: 288 h	Dilatometry, x-ray, DMA
Haidar et al. (1990)	PC	Temp.: 120 °C Time: up to 720 h	Dynamic tensile properties
Bertilsson et al. (1990)[4]	PC/PBT blend	Temp.: 130 °C Time: 0, 10, 1000 h	DMTA, density
Cheng et al. (1992)[5]	Mod. PC	Temp.: 125, 130, 135 °C Time: up to 1000 h	DSC, density, viscosity, DMTA, REM, tensile
Lundberg et al. (1995)	PC	Temp.: 22, 120 °C Time: up to 22 h	Tensile creep
Heymans (1996)	PC	Temp.: 30, 80, 120, 130 °C Time: up to 167 h	FTIR
Bauwens-Crowet (1999)	PC	Temp.: 23 °C Time: up to 10 years	DMA
Davis et al. (1998)	PC	Temp.: 30, 80, 120 °C Time: 0, 25–64 h	PALS
Heymans et al. (2002)	PC	Temp.: 25–60 °C Time: up to 312 h	FTIR
Dhara et al. (2009)[6]	PC block copolymer	Temp.: 120, 130 °C Time: up to 480 h	Impact, TEM, MFI
Pérez et al. (2009)	PC	Temp.: 50 °C Time: up to 600 h	DSC, TGA, MFI, tensile
Suzuki et al. (2012)[7]	PC blend	Temp.: 50–130 °C Time: up to 48 h	DMA, TEM
Redjala et al (2019)[8]	PC	Temp.: 120 °C Time: 72, 144, 216 h	TGA, DTA, FTIR, x-ray, hardness, compression, REM
Steiner et al. (1988)[9]	i-PP	Temp.: 90–120 °C Time: 48–168 h	DTA, tensile, IR- and DIA, diffusion
Horrocks et al. (1988)	PP	Temp.: 130 °C Time: 480 h	DTA, TGA
Fayolle et al. (2000)	i-PP	Temp.: 90 °C Time: up to 325 h	Molecular weight, FTIR, tensile
Schwarz et al. (2001)[10]	PP	Temp.: 20, 40, 60 °C Time: 5 min–3000 h	Tensile, DMA, DSC, density
Rincon-Rubio et al. (2001)	i-PP	Temp.: 110 °C Time: up to 35 h	Simulation
Fayolle et al. (2004)		Temp.: 70, 90, 110, 130 °C Time: up to 1300 h	FTIR, SEC, REM, tensile
Rjeb et al. (2005)[11]	PP	Temp.: 5–30, 45 °C Time: 1440, 1920 h	TG, DSC
Mowery et al. (2005)	PP	Temp.: 50, 80, 109 Time: up to 7200 h	Solid state NMR

TABLE 1 (Continued)

Author	Polymer	Aging	Investigations
Law et al. (2008)[12]	i-PP	Temp.: 90, 120 °C Time: 288 h	WAXS, FTIR
Mourad et al. (2010)[13]	PE/ PP blend	Temp.: 100 °C Time: 48, 96, 168, 336 h	Tensile, hardness, TGA
Lv et al. (2013)	PP	Temp.: 100 °C Time: up to 85 h	FTIR, DMTA, permeability, DSC, tensile
Horák et al. (*2015*)	PP	Temp.: 100 °C Time: 1600 h	Capacitance, voltage measurements

TABLE 2 Literature review for thermal-oxidative aged thermoplastic foams.

Author	Polymer	Aging	Investigations
Delabroye et al. (2005)[14]	PP	Temp.: 70, 150 °C Time: up to 1272 h	ASTM, density
Noble et al. (1984)[15]	PU	Temp.: 25 °C Time: $\sim$ 4394 h	ILD-testing, hardness
Ramesh et al. (2011)[16]	Silicon	Temp.: −36, 70 °C	Tensile, compression, creep
Smardzewski et al. (2012)[17]	PU	Time: 17520 h (730 days)	Compression
Yarahmadi et al. (2017)[18]	PU	Temp.: 150 °C Time: 1344 h	3-point bending, adhesion, FTIR, GC–MS analysis

block copolymer. Changes in impact behavior and yield strength were observed. Contrary to expectations, the impact strength of a sample aged at 130 °C was higher than at 120 °C. Redjala et al.[8] also noted an improvement in thermal stability, but the mechanical properties in the compression test decreased after heat treatment.

The literature on the subject of thermal aging of thermoplastic foams is limited, while a large amount of research has been reported for PU systems. The literature on thermal-oxidative aged thermoplastic foams and some selected papers on PU foams are discussed below (see Table 2). One of the few papers on this topic is the work of Delabroye et al. They investigated and patented a foam with densities around 8–192 kg/m^3, comprised of at least 50% PP and contains stabilizers and radiation blockers. They also investigated the foam stability of the resulting continuous extruded foams (aliphatic blowing agents) at 150 °C and were able to obtain foamed components that could withstand aging of up to 48 days.[14] Noble et al. discussed the influence of the environment and hence thermal aging on PU foams as early as 1984. The resistance to compression of the foams degraded continuously with aging time. However, the authors were not able to determine which relative influence was responsible for this degradation.[15] In addition, Yarahmadi et al. and Smardzewski et al. recently dealt with the influence of aging on PU foams. Smardzewski et al. found that aging had a negative effect on stiffness and that there was a decrease of 14%–27% depending on the

foam.[17] Yarahmadi et al. studied thermo-oxidative degradation of PU foams in air at 150 °C for 8 weeks. They determined that new carbonyl groups formed and CH_2 groups disappeared. Initially, it was observed that the mechanical properties could be maintained, but above a critical aging time, they started to detoriate linearly.[18] Ramesh et al. studied the temperature aging of silicone foam. As the aging temperature increased, the modulus also increased. However, no significant relationship was found between aging temperature and strain.[16]

To the best knowledge of the authors, there are no studies on the aging of bead foams, although foams such as EPP and EPS have been commercially available for a long time. EPC, on the other hand, is a completely new bead foam on the market (JEC World 2020 press release[i]). Until now, only the mechanical performance of EPC has been studied in comparison with EPP and EPET.[19] The aim of the work was to give an overview on the impact of thermo-oxidative aging of EPP compared with EPC on properties relevant to typical foam applications.

2 | MATERIALS AND METHODS

2.1 | Materials

The polycarbonate beads with a density of 150 g/L used for this study were based on a development grade

(CS-PCS-CVKKK-5-1286538830, Covestro Deutschland AG). These beads were manufactured in accordance with already reported process.[19]

EPP beads were selected as a reference material for comparison reasons (Neopolen HD 130, Density of 130 g/L from BASF SA) was also molded at Neue Materialien Bayreuth GmbH (NMB) under appropriate molding conditions (best part quality) into parts with a density of 200 ± 10 kg/m^3 and used for this characterization.

2.2 | Experimental

2.2.1 | Final part preparation

The steam chest molding (SCM) of the beads was carried out with a high-pressure Steam-Chest-Molding Machine (TVZ162/100PP for EPC and Transtec72/52PP for EPP both from Teubert Maschinenbau GmbH). The density of the molded parts ($300 \times 200 \times 15$ mm^3) was 200 ± 10 kg/m^3. The required pressures were in the range of 10 bar for EPC and 4–5 bar for EPP. The steam temperature was around 180 °C for EPC and 140–145 °C for EPP. After molding the parts were dried in oven at 60 °C for 24 h.

2.2.2 | Material characterization

Aging of the final parts was performed on already prepared test-specimen of geometries described below. The specimen were prepared with water-jet cutting. The samples were aged in a convection oven (Modell UN110plus, Memmert GmbH + Co. KG) at temperatures of 110, 120, 130 and 140 °C over periods of 0 (reference), 100, 500, 750 and 1000 h. The temperatures were chosen around the continuous service temperature of EPC ($\sim$130 °C) as well as EPP (range between $\sim$90–120 °C).

The foam morphology of the aged samples was investigated with a scanning electron microscope (JEOL JSM-6510) with an acceleration voltage of 10 kV and a secondary electron (SE) detector. The samples were cut with a fresh razor blade and sputtered with a 13 nm thick gold layer. Evaluation of cell diameters and cell size distribution was performed with the freeware program (ImageJ, NIH) on an average of at least 200–400 cells for EPC and due to higher inhomogeneity 300–600 cells for EPP.

Density was determined with a scale and a density tool according to the Archimedes' principle (AG245, Mettler/Toledo). Each aged sample group was measured multiple times to obtain a standard deviation. Skinned 3-point bend samples were generally used for this examination. DSC measurements (DSC1, Mettler Toledo) were performed to detect the oxidation onset temperature (OOT) according to

the standard ISO 11357-6:2018. Samples of about 10 mg were placed in standard aluminum pans. Tests were carried out with different heating rates β of 5, 10 and 20 K/min under air atmosphere. The start of the oxidation reaction was determined as an exothermal deviation in the heat flow.

Post-aging characterization by DMA was performed (Gabo Eplexor 500 N, NETZSCH GmbH & Co. Holding KG) in compression ($15 \times 15 \times 15$ mm^3 specimen) at a temperature range from -25 to 250 °C, a heating rate of 1 K/min, a strain-controlled mode with an amplitude of 5% (static) and 2% (dynamic) of the sample height at a frequency of 1 Hz.

For further characterization of the final parts, compression tests and 3-point bending investigations were performed at room temperature. Tensile measurements were not carried out intentionally, since the results from three-point bending experiments are more reliable, as shown in our previous research[19] and as the failure of the specimen is anyway determined by tension. Compression testing was performed according to DIN EN ISO 844. According to the standard, the specimen geometry was scaled to 15 mm^3 ($15 \times 15 \times 15$ mm^3) and the test speed was scaled to 5 mm/min on a universal testing machine (Zwick Z020) equipped with a 10 kN load cell up to 60% compression. 3-point bending tests were carried out based on ISO 1209-1 with the same testing machine at 10 mm/min and with a 20 kN load cell. The outer layers of the specimen were removed prior to aging to suppress the influence of the skin layer. The specimen geometry was modified to $120 \times 25 \times 10$ mm^3. Impact tests were conducted at RT (falling dart) in accordance to DIN EN ISO 6603-2 by the use of a falling weight impact tester (Fractovis Plus, Instron) with an energy of 40 J and an impact velocity of 4.4 m/s and $60 \times 60 \times 15$ mm^3 specimen. All mechanical investigations were performed at room temperature with specimen of same part density around 200 kg/m^3.

Thermal conductivity measurements were carried out with a black-box device (HFM 446 Lambda, NETZSCH GmbH & Co. Holding KG) at -10, 10, 25, 50 and 70 °C with a specimen geometry of $200 \times 200 \times 15$ mm^3.

3 | RESULTS AND DISCUSSION

3.1 | Density, foam morphology and oxidation stability of aged EPC and EPP parts

Before further characterization, the aged plates were subjected to a density and morphology study, to investigate how aging affects the foams density and morphology. Figure 1 shows the material density as a function of the aging time.
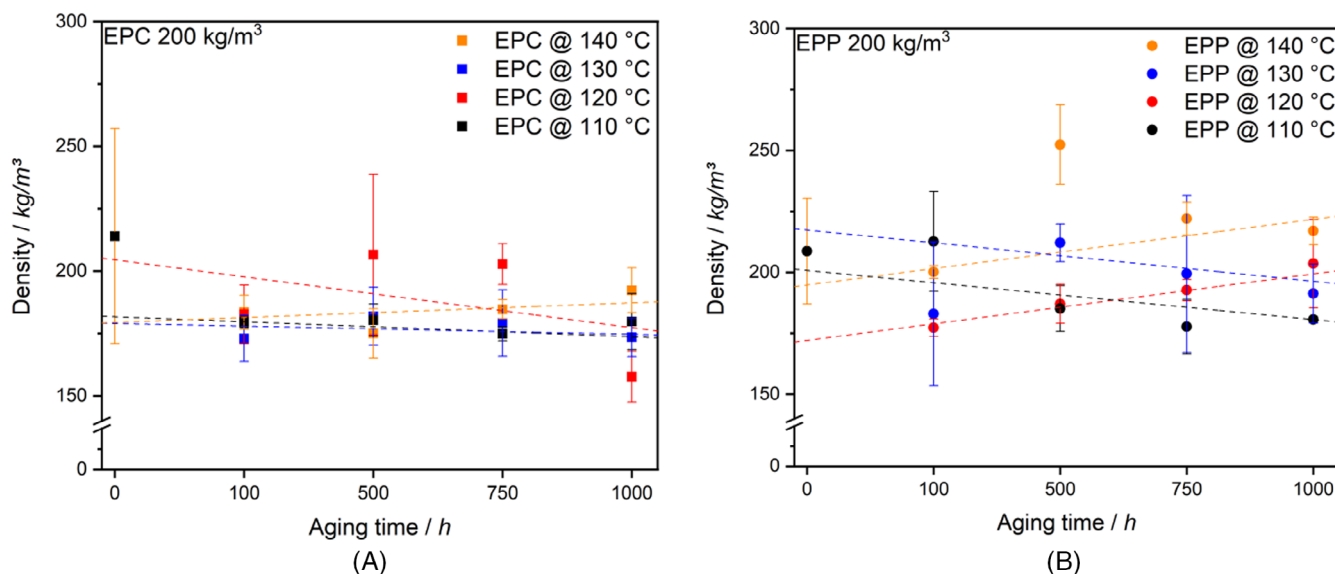
FIGURE 1 Density of EPC and EPP parts as function of aging time (0–1000 h at 110, 120, 130 and 140 °C).
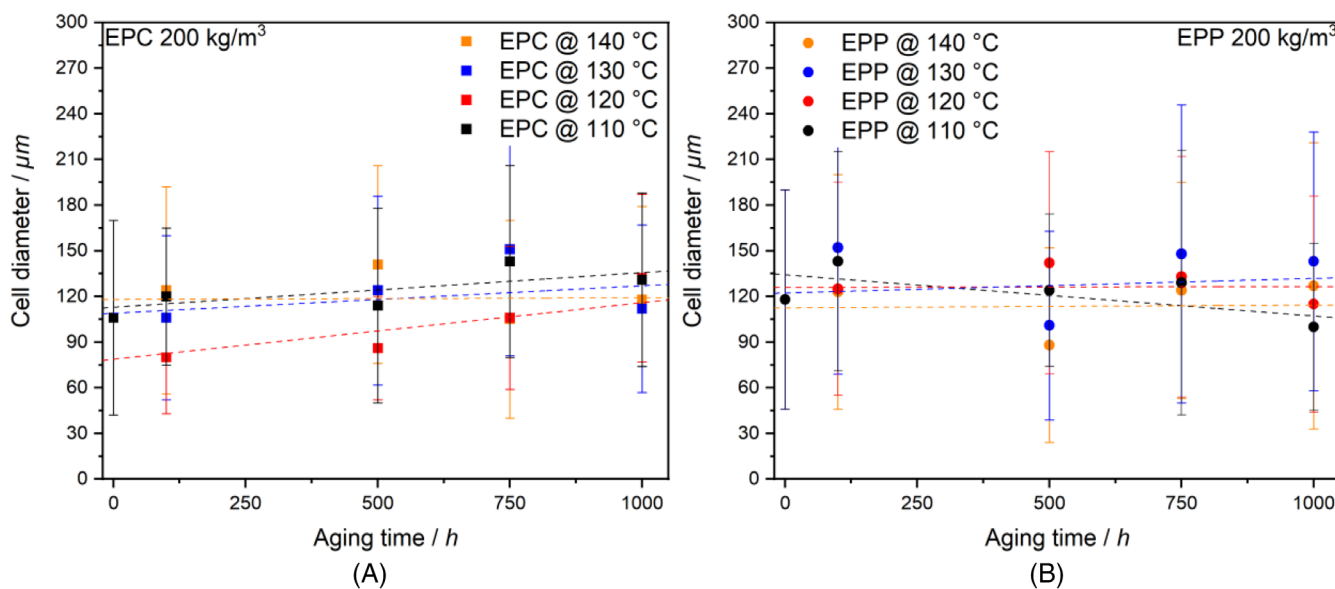

FIGURE 2 Average cell diameter of EPC and EPP parts as function of aging time (0–1000 h at 110, 120, 130 and 140 °C). The error bars do not represent the margin of error but the width of the distribution of the cell size.

For EPC, aging up to 100 h results in a 9%–14% decrease in part density regardless of aging-temperature, indicating an expansion of the parts. Further increasing the aging-time to 500 h shows no significant effect as the values are almost within the measurement error. After 1000 h of aging, on the other hand, the density starts to vary less. Nevertheless, all aged samples show a decreased density compared to the unaged samples, thus showing a general trend towards lower densities due to aging. As with EPP, the density decreases with 100 h of aging even at lower aging temperatures. Only further aging at 110 °C leads to lower part densities. Higher

aging temperatures lead to a constant or rather increasing foam density despite a certain deviation. If the foam morphology is taken under consideration (Figure 2), in combination with the density effects, the aging mechanisms of EPC and EPP becomes visible. For EPC thermal aging leads to an increase in the average cell diameter by maximum 42% (from 106 ± 64 to 151 ± 70 μm). There is an increasing trend in the density despite values that are within the margin of experimental error. The increase in the average cell volume from 444 to 503 μm^3 occurs after only 100 h of thermal treatment at 110 °C and correlates well with the decrease in density. Here, an increasing
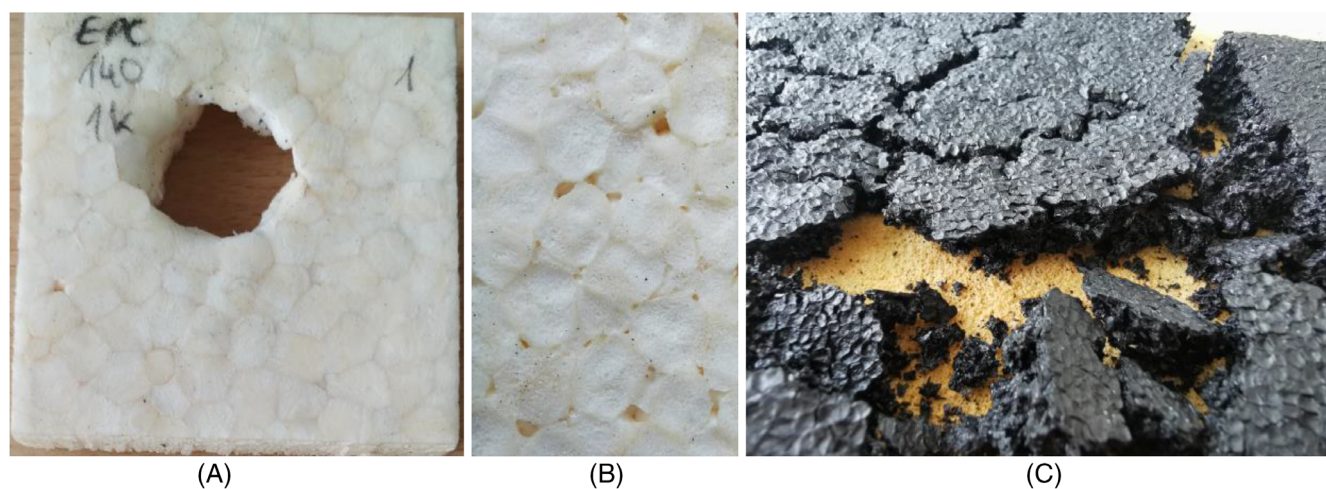
FIGURE 3 Aged samples after 1000 h at 140 °C of (A) unskinned EPC, (B) skinned 3-PB sample and (C) EPP.

trend of the average cell volume with increasing aging time up to 1000 h at 110 and 120 °C can be observed. At higher aging temperatures, the cell volume starts to decrease after aging from 500 to 750 h (from 633 to 469 μm^3 after 750 h at 130 °C).

Especially at the highest aging temperature of 140 °C, it becomes apparent after 750 and 1000 h how EPC reacts to thermal aging. Up to a temperature of 135 °C the material shows no significant reaction to thermal aging. At higher temperatures and storage times (140 °C after 500–750 h), EPC loses its dimensional stability (Figure 3A). The individual beads shrink, which leads to an overall reduction in the contact area between the beads (Figure 3B). This process is accelerated when the aged sample does not have a compact skin. The foam cells shrink and show a higher number of ruptured damaged cells in the SEM. This also results in an increase in density. In contrast, a much greater variation in cell morphology is found in EPP (Figure 2B) due to the inhomogeneity of the beads (e.g., 118 ± 71 μm in the unaged sample and 127 ± 94 μm after 1000 h at 140 °C). Some of the beads have a very coarse morphology, while others have a homogeneous and small cell size distribution. On this basis, a trend statement is rather difficult. It is assumed that the average cell diameters of EPP do not change much during aging and are within the range of experimental deviation. Combined with a trend of increasing density caused by thermal oxidative aging, EPP seems to express a different aging mechanism. In EPP, thermal treatment causes two effects. First, the semi-crystalline EPP which was annealed during batch foaming (perfection of the crystalline structure) shows a decrease in crystallinity at lower aging temperatures. At higher aging temperatures (130 and 140 °C) the EPP starts to post-crystallize (Table 3 in Data S1) which leads to a certain increase in mechanical properties

(e.g., bending modulus), but also to stiffening of the material. The second effect is a solidification of the outer surfaces of the specimen with a more or less steady trend in the average cell size. The latter leads to a highly visible increase in broken cells during aging in SEM, hence the increase in density.

As can be seen in Figure 3, the thermo-oxidative stability of EPC and EPP at 140 °C is vastly different resulting in a strong embrittlement of the colored EPP during aging in contrast to EPC. This embrittlement of EPP is mainly caused by oxidation. Therefore, the oxidation resistance of the material was determined by measuring the oxidation onset temperature via DSC (OOT).[20,21] Using the Kissinger method, the activation energies of oxidation were calculated from the slope of the curve (Figure 4).

Here, EPC has an activation energy of 239 kJ/mol, which is 2.5 times the activation energy of EPP with 97.2 kJ/mol. This explains the lower oxidation resistance of EPP compared with EPC, which is consistent with the literature where values of 50,[22] 115[23] and 124 kJ/mol[24] were found for compact polypropylene and values of 213 kJ/mol for compact polycarbonate. The higher value of EPC can be explained by the aromatic structure of EPC, which is generally less susceptible to oxidation.

4 | INFLUENCE OF THERMO-OXIDATIVE AGING ON MECHANICAL PROPERTIES

4.1 | Comparison of dynamic-mechanical analysis of aged EPC and EPP

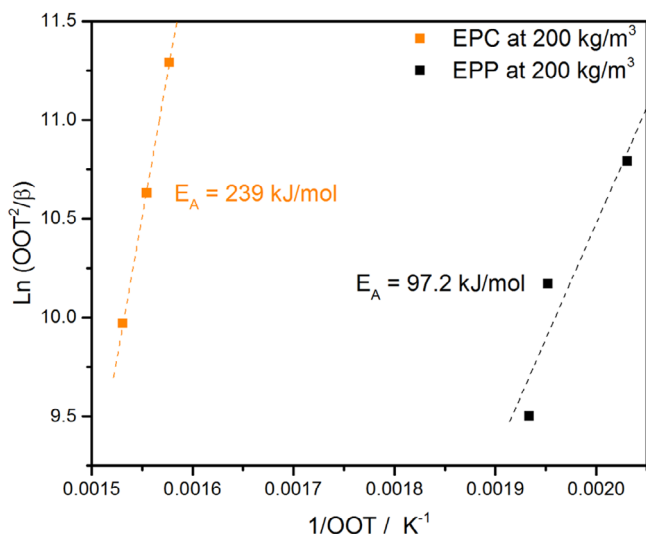DMA temperature sweeps in compression were performed for EPC and EPP on thermo-oxidatively aged

FIGURE 4 Kissinger Plot of obtained OOT values of EPC and EPP.

samples, aged up to 1000 h at different temperatures. Their performance is compared with that of the neat bead foam part and then with each other. In Figure 5 the diagrams show the influence of 100 and 1000 h aging on the storage modulus of EPC and EPP.

Neat EPC part exhibits a profound thermal history, which shows in form of an increasing storage modulus upon temperature increase. A maximum modulus of 58 MPa was observed, before the modulus drops at the glass transition of 144 °C. Thermal treatment for 100 h at 110 °C leads to a significant increase in modulus of almost 27% (74 MPa) for the EPC part through annealing, as well as at 120 °C with a similar storage modulus as the reference material. Aging at higher temperatures for 100 h lead to a generally lower storage modulus. As for EPP in Figure 5B, thermal treatment for 100 h leads to a decrease in thermo-mechanical performance as the storage moduli decrease with higher aging temperatures.
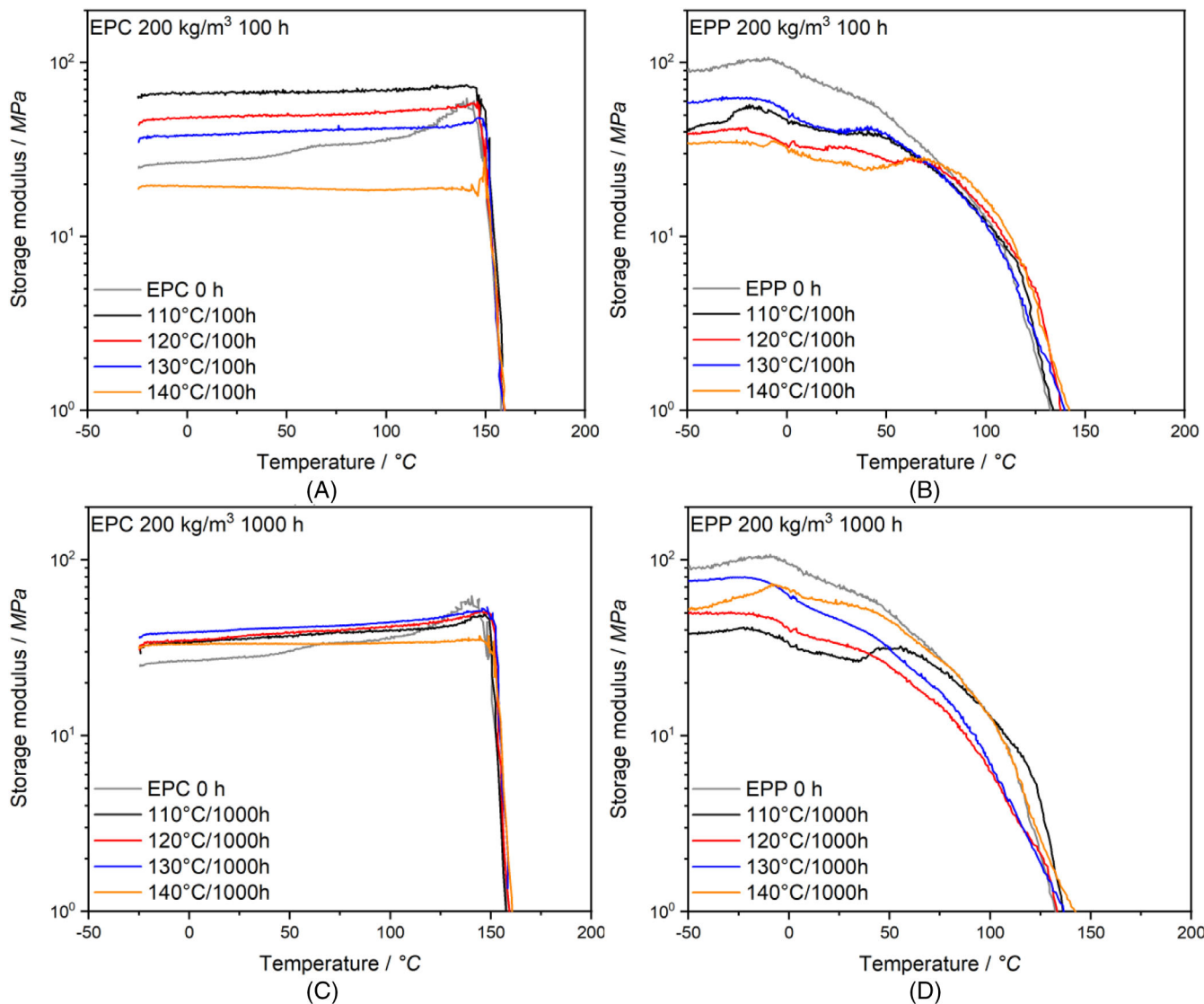

FIGURE 5 DMA temperature sweep (1 K/min) for EPC and EPP bead foam parts at 200 kg/m³.

Considering the measurement data scattering, the performance of the EPP part can be considered similar after aging temperatures of 110, 120 and 130 °C. Aging for 100 h at 140 °C results in the lowest values for EPP with a storage modulus around 34 MPa (plateau value) in comparison to the unaged EPP sample with 103 MPa.

After aging the EPC samples for 1000 h, the material behavior in the DMA changed (Figure 5C). The storage moduli of the aging-temperatures of 110, 120 and 130 °C can be considered similar (48–51 MPa) and perform slightly under the maximum value of the unaged EPC curve (58.4 MPa), but significantly worse that the 100 h specimen. The performance of EPC after aging at 140 °C for 1000 h is higher compared to the same aging temperature after 100 h (Figure 5A) with a storage modulus of 19 MPa. Thus, it is clear that EPC starts to shrink (significantly more on areas without the outer layer), hence the drop in performance which is compensated by a densification of the sample (Figure 3A,B). On the other hand, EPP samples show a densification as well. Here, an increasing aging-temperature leads to higher storage moduli values (at −10 °C) of 38 (110 °C)–74 MPa (130 °C) while the samples increasingly deteriorate (Figure 5D). The samples for 1000 h at 140 °C as well as at 130 °C are strongly charred and brittle (130°C rather on the outside) and crumble apart by application of higher pressures. In conclusion, it is visible that EPC is rather insensitive to thermal aging at temperatures up to 130 °C and 1000 h. It retains good dynamic-mechanical properties, which begin to decrease above temperatures of 140 °C. EPP on the other hand loses around 68% of the modulus already after 100 h at the lowest temperature of 110 °C and hence is prone to thermal-oxidative aging.

4.1.1 | Effect of aging on the compressive properties of EPC and EPP molded parts

Polymer foams are often subjected to compressive loading. Therefore, it is important to understand how thermal aging affects mechanical performance under this loading condition. EPC is a bead foam for higher temperature applications up to 135 °C, while EPP can be used up to 110 °C, according to manufacturers. The comparison of the compression modulus after aging of the two materials is summarized in Figure 6.

The unaged compression modulus of EPC is 49.7 ± 5 MPa. Aging between 110 and 130 °C leads to a constant compression modulus around 50 MPa with a trend towards higher values with increasing thermal-oxidative aging. At a temperature of 140 °C this trend changes. The samples show some shrinkage and color change, while the compression modulus shows a downward trend. Nevertheless, the decrease in modulus represents only 17.5% for a thermal aging of 1000 h at 140 °C. As for EPP, the unaged compression modulus is comparable to EPC with a value of 52 MPa, but it shows a significantly higher temperature/aging sensitivity. Figure 6B shows a general trend of decreasing modulus with increasing aging time and aging temperature. At aging temperatures of 110, 120 and 130 °C, EPP loses 31%, 38% and 25% respectively, over the course of 1000 h aging. Aging at 140 °C leads to increased thermal decomposition after 500 h, resulting in a 84% decrease for 750 h and 95% for 1000 h. These EPP samples deteriorate severely and became rather charred as well as challenging to test. The slightest stress leads to complete crumbling of the specimen.
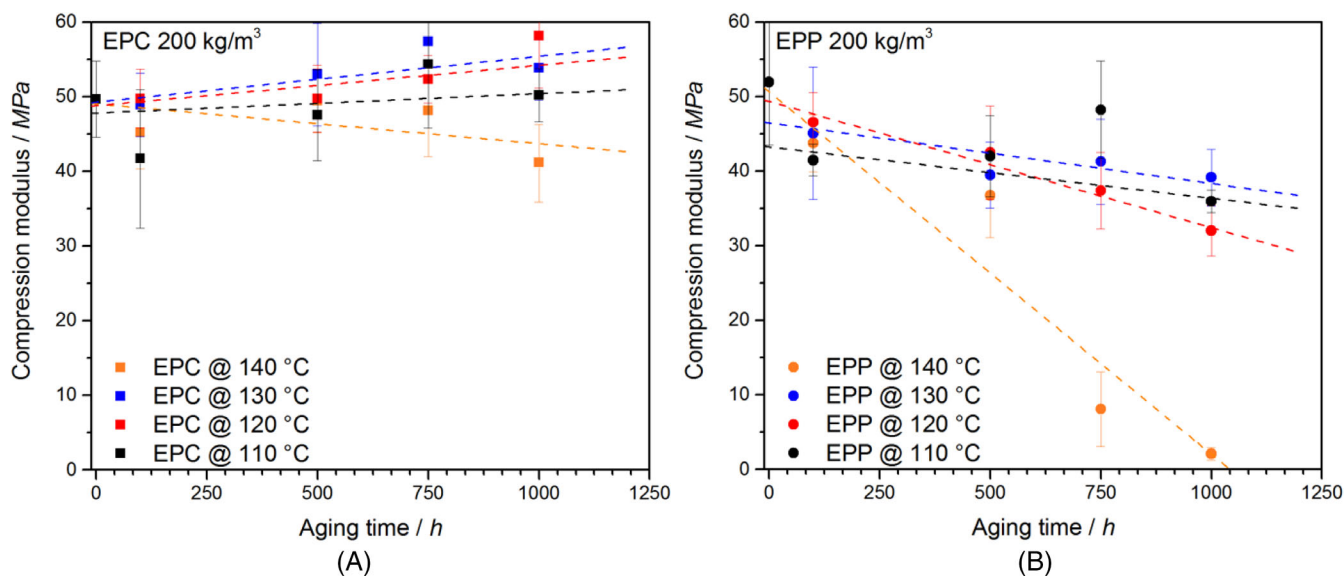

FIGURE 6 Comparison of compression modulus of EPC (A) and EPP (B) after 100–1000 h aging at 110, 120, 130 and 140 °C.
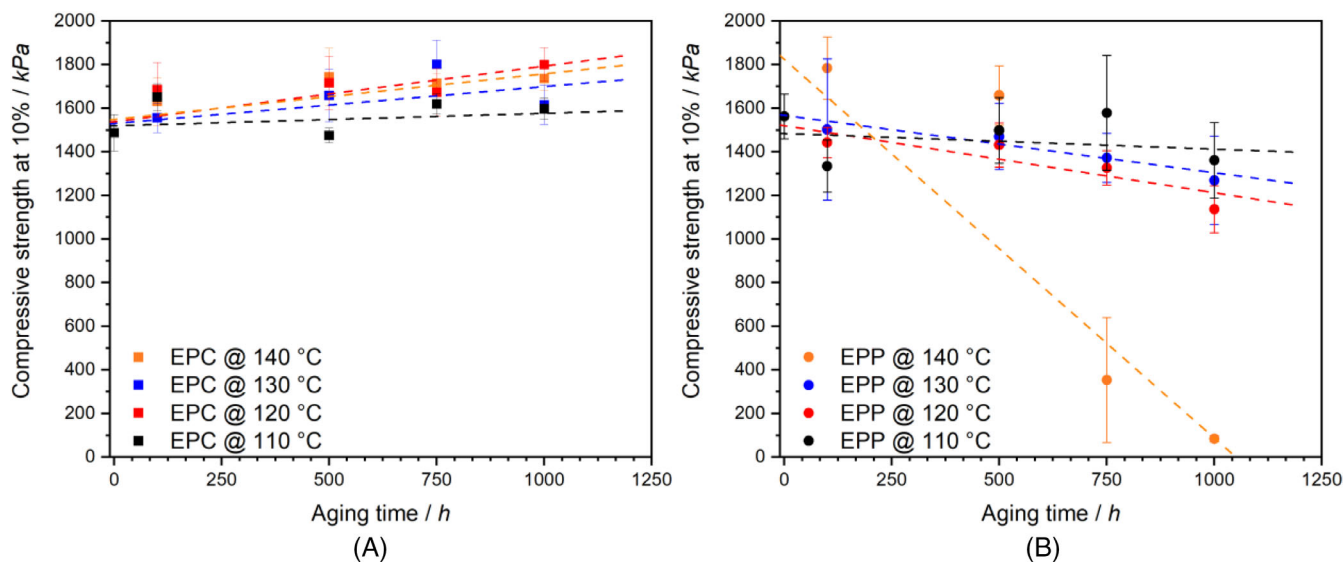
FIGURE 7 Comparison of compression strength of EPC (A) and EPP (B) after aging 100–1000 h at 110, 120, 130 and 140 °C.

Another important key value for compressive performance, compressive strength, is investigated at a compression of 10% in Figure 7A,B. A general trend of a slight increase over aging time and temperature can be observed for EPC, as well as a temperature/aging-insensitivity of the compressive strength, as it exhibits the same value around 1.7 MPa within the experimental deviation (Figure 7A). Nonetheless, 100 h of thermal treatment increases the compressive strength of EPC from 1.5 to 1.7 MPa (13% increase). This can be attributed to a higher polymer strength induced by further stretching of foamed cells through aging.[25] For EPP on the other hand, a decreasing trend, similar to the behavior of the compression modulus, can be observed (Figure 7B). The compressive strength decreases over the aging time and an increasing aging temperature from 1.6 MPa (unaged) to the lowest value of 1.1 MPa for 1000 h at 120 °C (31% drop). The aging temperature of 140 °C shows a densification (stronger on skinned areas) in the samples, which first result in an increase of compressive strength by 13%, but significantly drop to 0.4 MPa (750 h) and 0.08 MPa (1000 h) due to thermal decomposition. This represents a loss of 95% of the compressive performance (1000 h at 140 °C) for EPP. Thus, the potential and insensitivity of EPC to thermal-oxidative aging for structural applications is evident compared to EPP. The full precise data can be found in Table 4 of Data S1.

4.1.2 | Effect of thermal aging on bending properties of EPC and EPP final parts

Bending is another type of loading to which polymer foams are subjected in many cases. It represents a complex loading in which the upper side is subjected to a compressive loading and the bottom surface is subjected to tensile loading. Flexural tests allow an indication of the bending stiffness of the part and the welding quality, which is represented by the maximum bending strain and strength. This is the first time that the influence of thermal-oxidative aging on the bending properties of a bead foam has been reported in the literature. EPC exhibits in Figure 8A–D an unaged bending modulus of 48 ± 10 MPa. This value does not change significantly with aging temperature or aging time, deviating only within the margin of error. A maximum value of 52 ± 3 MPa (130°C, 1000 h) and the lowest value 45 ± 3 MPa (140 °C, 500 h) were determined, although the general trend in Figure 8A is slightly upward. The bending strength of EPC increased by 11%–21% compared to the unaged value of 1.9 MPa. Moreover, the aged values for bending strength of EPC range in the area of 2.1–2.3 MPa, confirming the insensitivity of EPC to thermal-oxidative aging (Figure 8C).

EPP, on the other hand, has a higher unaged bending modulus of 66.9 MPa, but is more sensitive to thermal treatment. Aging at 110 and 120 °C leads to a decreasing general trend in bending modulus with a drop by 10%–19% (Figure 8B). At higher temperatures of 130 °C, EPP begins to solidify at the surface of the specimen and experience increased post-crystallization (Table 3 in Data S1), leading to an increase in the bending modulus by 12%. Further increase in aging temperature leads to an unprecise trend due severe degradation of the specimen. The EPP specimen aged for 1000 h at 140 °C was so brittle, that no testing was possible. Nevertheless, this value should be expected to be very low, indicated by the other aged mechanical results. As for the bending strength of EPP, the general trend shows that aging leads to an
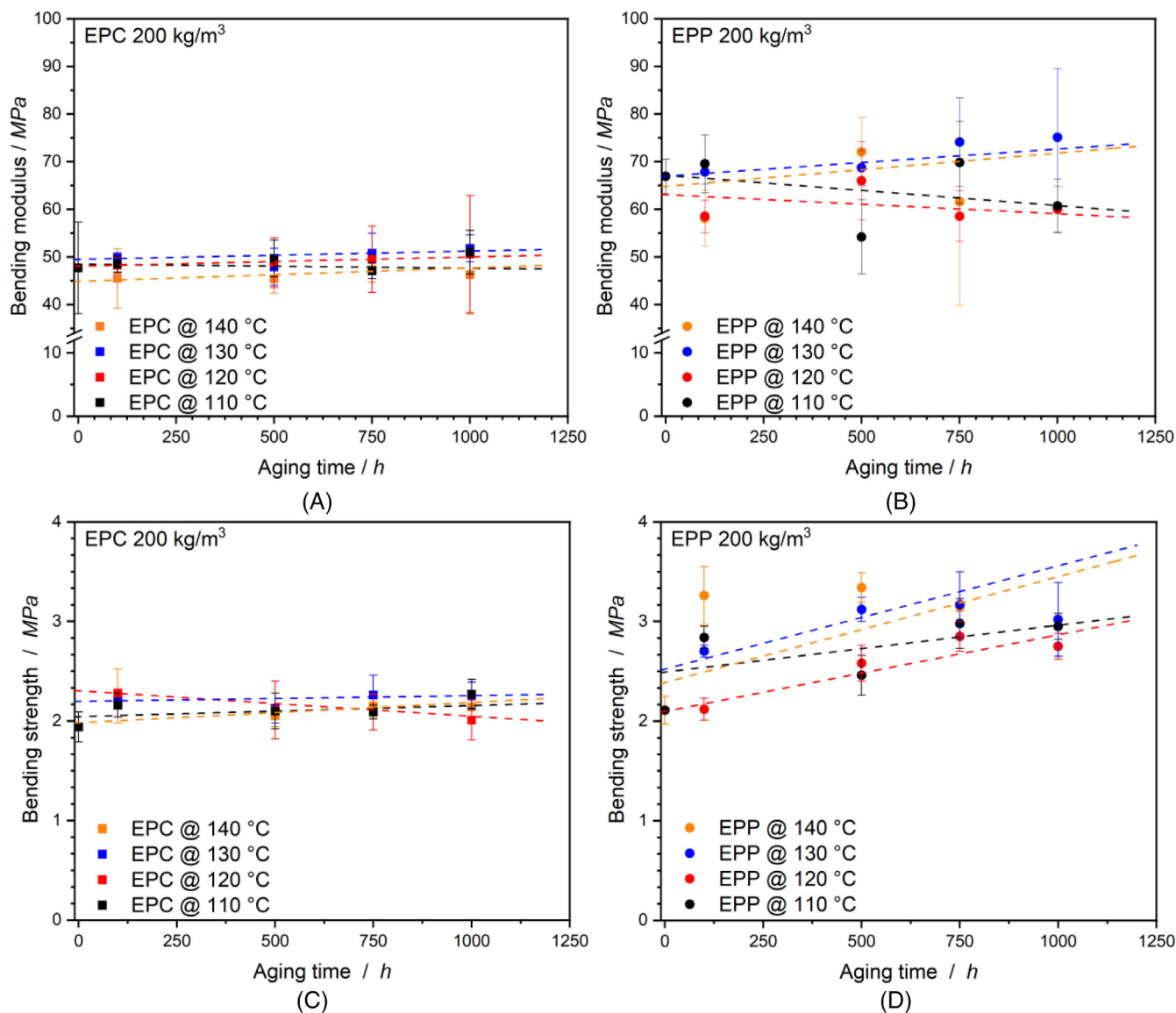
FIGURE 8 Comparison of bending modulus of EPC (A) and EPP (B) after aging 100–1000 h at 110, 120, 130 and 140 °C.*EPP after 1000 h at 140 °C not measurable.

increase in bending strength. Even aging at 110 °C for 100 h leads to a 33% value increase, which is caused by the consolidation/densification of the specimen's skinned surface (Figure 7D). Higher aging temperatures enhance this effect with a maximum measured bending stiffness of 3.3 MPa (+57%) for 500 h at 140 °C.

Furthermore, it was possible to investigate the influence of the thermal-oxidative aging on the welding quality/strength. Here, the welding strength is expressed by the *bending strain at maximum stress* and compared for aged EPC and EPP in Figure 9. The *bending at break* sometimes needs to be manually adjusted in the software, while the *bending strain at maximum stress* is a fixed value, which can be reliably determined by the software. The aging mechanism for the amorphous EPC is the

contraction of the oriented polymer chains, once the system gets enough energy to plasticize as evidenced by specimen shrinkage. This negatively influences the bonds between the welded beads, thus lowering the welding quality. The thermal aging of EPC leads to a decreasing general trend in the *bending strain at max. stress*. At lower aging temperatures the drop in *bending strain at max. stress* (representing welding quality) deviates between 11% and 20%. This effect is most pronounced at higher temperatures above 130 °C, with the lowest value of 7.7% (− 22%) after 1000 h at 140 °C, where the samples even become discolored. For EPP on the other hands, two different effects influence the values. The first effect is the surface consolidation of the specimen, which is counteracting the embrittlement. It causes a more plastic
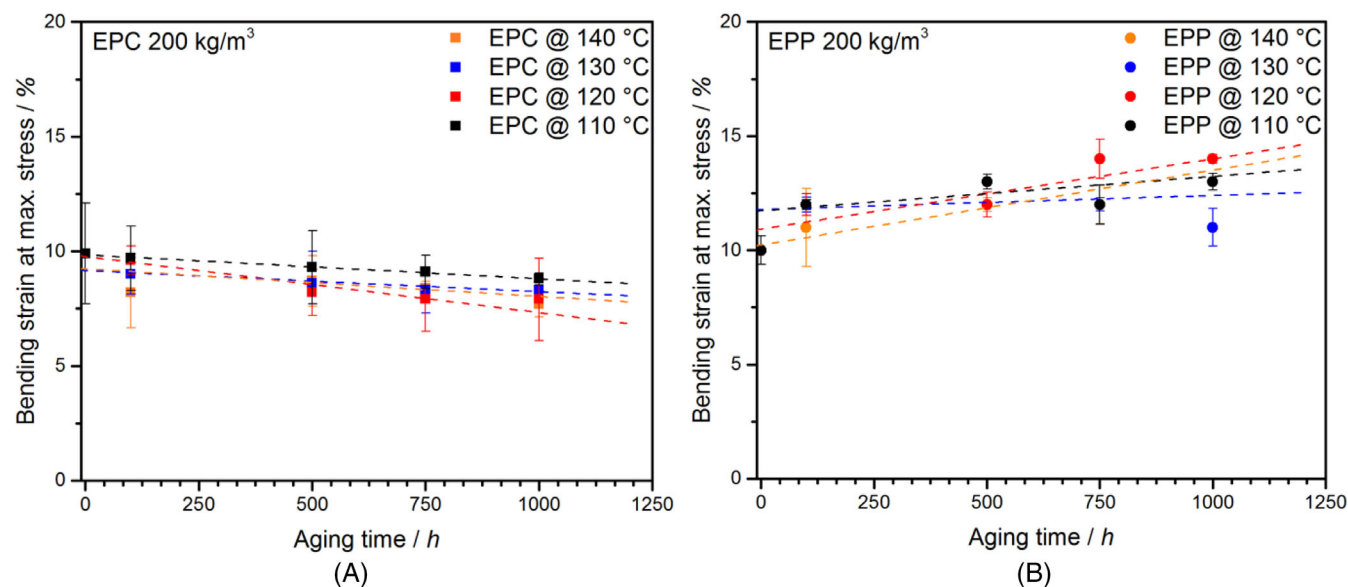
FIGURE 9 Comparison of *bending strain at max. stress* of EPC (A) and EPP (B) after aging 100–1000 h at 110, 120, 130 and 140 °C. *EPP after 1000 h at 140 °C not measurable.

response of the material and thus higher bending strain values. The second effect is caused by heat-treatment of EPP. At lower temperatures, a decrease in crystallinity is caused by disruption of the perfected crystalline structure during the annealing step (batch foaming). Higher temperatures on the other hand enable a post-crystallization in EPP (Table 3). This increases the degree of crystallinity of EPP but makes the material more brittle. At lower aging temperatures of 110 and 120 °C the post-crystallization is reversed/reduced, and the effect of surface-consolidation is more pronounced, leading to increasing trend in strain-values from 10% (unaged EPP) up to 14% (+ 40%) for 1000 h at 120 °C (Figure 9B). At aging temperatures of 130 and 140 °C the rate of post-crystallization increases and overtakes the consolidation of EPP samples. The latter even goes so far, as to cause the surface to become brittle and show fissures, leading to generally higher values than for neat EPP, but lower values compared to other aging temperatures. Precise and full data is summarized in Table 5 in Data S1.

4.1.3 | Effect of thermal aging impact-behavior of EPC and EPP final parts

This characterization investigates the effect of thermal-oxidative aging on the impact performance of the bead foams EPC and EPP. This mechanical test allows conclusions to be drawn about the force required for puncturing the foam (Figure 10) and the energy absorbed (Figure 11). The latter is defined by the area enclosed

beneath the corresponding impact curve. In Figure 10A, the influence of thermal aging time and temperature on the impact force for EPC is plotted. It can be observed, that the thermal aging process at temperatures between 110 and 140 °C up to 1000 h does not significantly influence neither the impact force nor the piercing force for EPC. The values after aging differ by 1.7 ± 0.2 kN and 0.9 ± 0.1 kN, respectively, compared to the unaged EPC. For EPP, a similar trend can be confirmed. The aged samples at 110–130 °C for up to 1000 h are around the values of the unaged EPP for impact force and piercing force with 1.5 ± 0.2 and 0.8 ± 0.1 kN, respectively (Figure 10B). In contrast, the aging of EPP at 140 °C shows a similar decreasing trend as in other investigations. After an aging time of 500 h, the mechanical performance of EPP decreases by 27% (750 h) and almost disappears after 1000 h with a decrease of 96%.

The influence of thermal aging on the absorbed impact energy of EPC and EPP can be observed in Figure 11A,B. Considering the unaged value for EPC of 22.7 ± 3 J, the aging leads to a minor decreasing trend in absorbed energy. The review of the complete data in Table 6 in Data S1 shows that the aging at 110–130 °C up to 1000 h decreases the absorbed energy values by 4%–25% compared with the neat EPC, but the values deviate in general in a similar area around 20 ± 3 J. Aging at the temperature of 140 °C shows a stronger influence on the absorbed energy and leads to a stronger decreasing trend with a drop by 27% after 1000 h of thermo-oxidative aging. Nevertheless, the aged values of EPC exceed the best performance of EPP. As displayed in
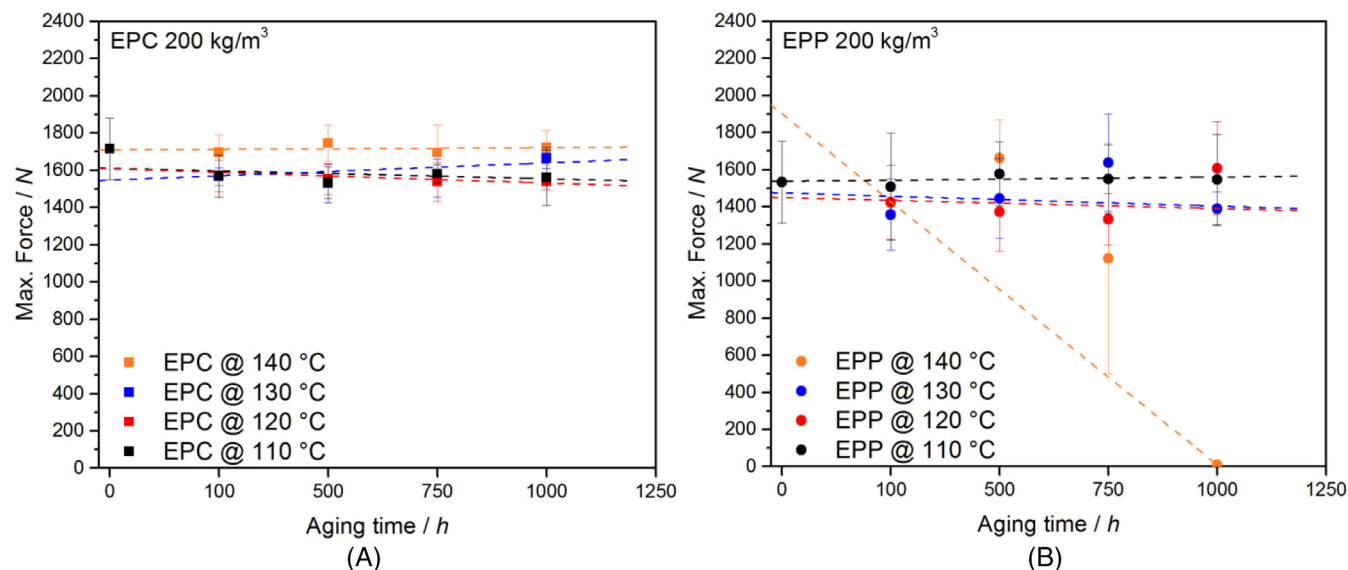
FIGURE 10 Comparison of max. force during penetration of EPC and EPP aged for 100–1000 h at 110, 120, 130 and 140°C.
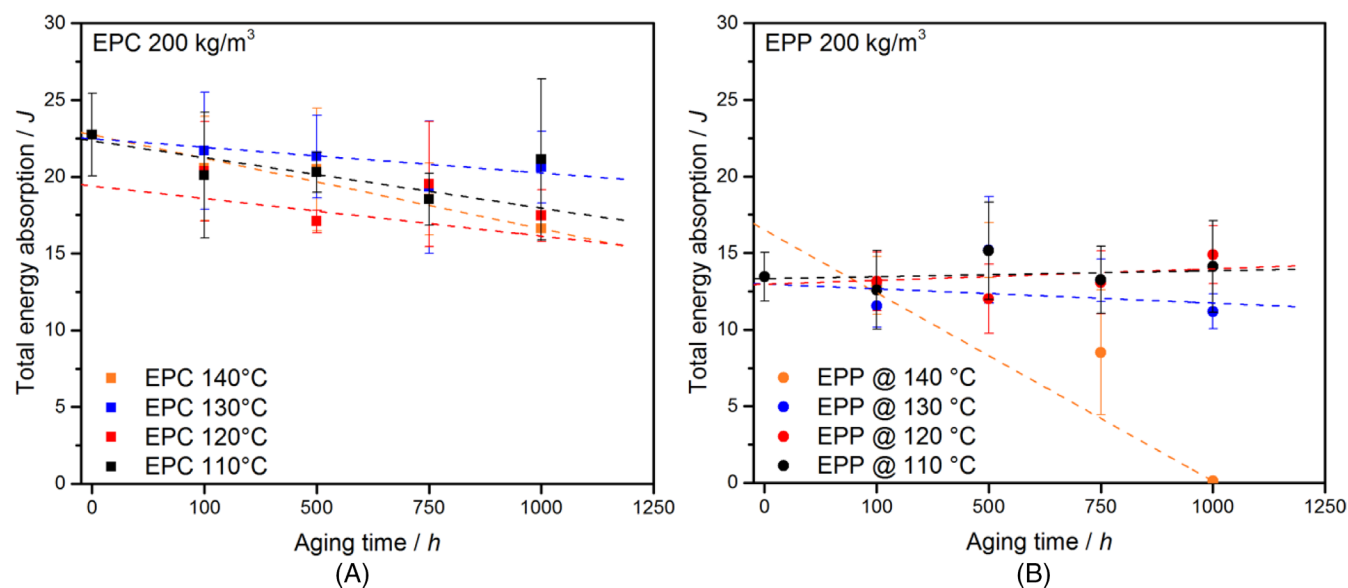

FIGURE 11 Comparison of total energy absorption of EPC and EPP aged for 100-1000 h at 110, 120, 130 and 140 °C.

Figure 11B, the absorbed energy of thermally aged EPP varies in the range of −17/up to +13% for the aging temperatures of 110–130 °C based on the unaged value of 13.5 J. Thus, no statement about the general trend is possible. At an aging temperature of 140 °C, the decreasing trend in Figure 11B becomes more pronounced with a drop in absorbed energy after aging 750 h by ∼40% and a strong decrease by 99% after aging for 1000 h at 140 °C. This result shows that the thermal aging of bead foams does not affect the impact performance in a strong way, as long as the foams do not degrade. Furthermore, the higher impact performance of EPC compared to EPP is confirmed, even after severe aging. The detailed data for this comparison can be found in Table 6 of Data S1.

4.2 | Influence of thermo-oxidative aging on thermal conductivity of aged EPC and EPP final parts

Insulating ability is another important property of foams. During use, for example, as a thermobox or in a near-engine application, the insulating material is repeatedly exposed to elevated temperatures for certain amount of
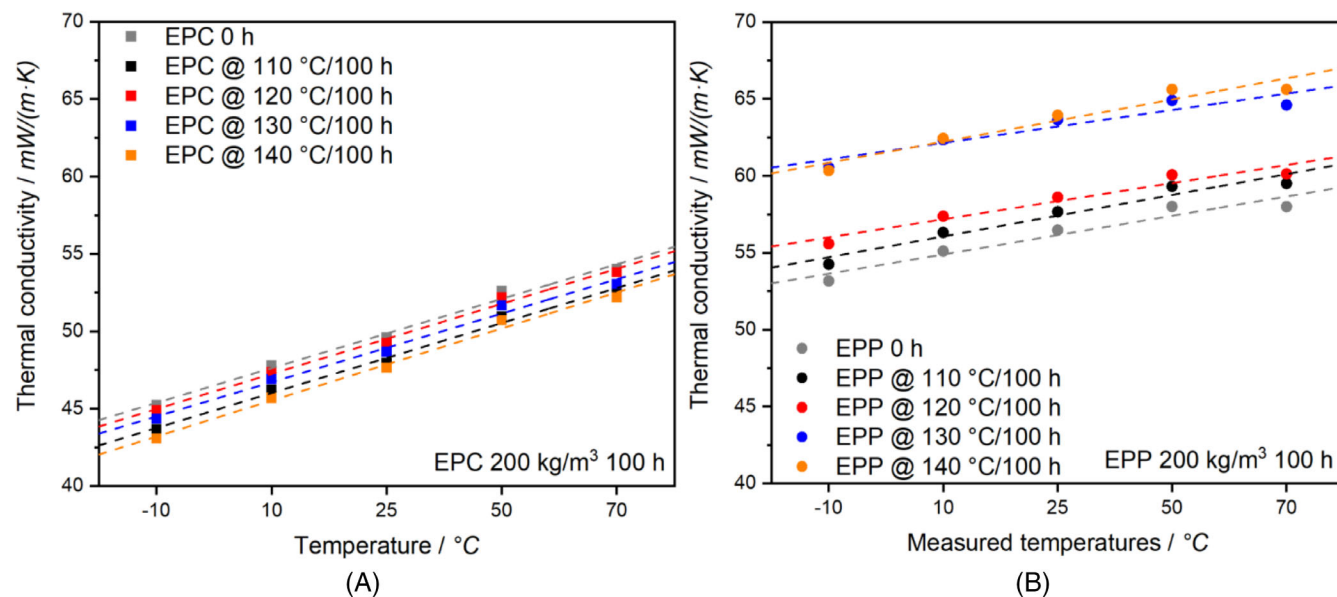
FIGURE 12 Temperature-dependent thermal conductivity of aged EPC and EPP for 100 h at 110–140 °C.

time. How this affects material performance and insulating capabilities has not been studied in the case of EPP and EPC. Therefore, both bead foams were investigated for their thermal conductivity at different temperatures (−10 to 70 °C) before and after aging. Figure 12A shows a linear correlation between the thermal conductivity and temperature for EPC. The most important factors affecting thermal conductivity are foam density and morphology. Here, thermal aging of EPC for 100 h results in a decrease in density of about 14%, which correlates very well with a decrease in thermal conductivity at all aging and measurement temperatures. The lowest thermal conductivity of 45.5 mW/(m*K) (10° C) is observed after aging at 110 °C for 500 h and represents a decrease by 5% compared with the unaged EPC. The positive contribution to this effect is a decrease in density which is offset by a small increase in cell sizes. This trend is reversed for EPP (Figure 12B). The unaged sample exhibits the lowest thermal conductivity of 55.1 mW/(m*K), while a heat treatment of 100 h at 110–140 °C leads to an increase of 2%–13%. Moreover, a correlation is observed between the increase in aging temperature and the increase in thermal conductivity of the samples. This correlates with the aging mechanism of EPP. Despite a slight decrease in the final part density during aging, the cell structures of EPP show an increasing cell diameter (cell collapse and coalescence) as the aging process progresses. This effect can be deduced by the average cell size and its deviation increasing from 118 ± 72 µm for unaged EPP to 127 ± 94 µm for 1000 h aged EPP at 140 °C. The later leads to a deterioration of the insulation properties in combination with the solidification of the

outer layer (neat thermal conductivity of PP around 170–220 mW/(m*K)[19]).

The longest aging time of 1000 h at 110–140 °C is examined in Figure 13. Here, the aging of EPC generally results in lower thermal conductivities. An aging temperature of 110 °C results in the lowest values of 45.8 mW/(m*K), while higher temperatures (130–140 °C) lead to comparable values. For EPP, the effect already observed is similarly pronounced after 100 h. Increasing the aging temperature after 1000 h leads to an increase in thermal conductivity, although the aging temperature of 140 °C is no longer measurable due to the decomposition of the final part.

To provide a more accurate indication of the effect of thermal aging on thermal conductivity, Figure 14 plots the conductivity of EPC and EPP at 10 °C as a function of aging time. The values at 10 °C were chosen for this comparison, because the material suppliers usually provide values for thermal conductivity at 10 °C. For EPC, it can be observed that thermal aging leads to a slight decrease in thermal conductivity at temperatures of 110–130 °C up to 1000 h. At an aging temperature of 140 °C this trend changes after 100 h and the conductivity values increase with aging time as the samples start to shrink (density increase) and the foamed cells are damaged during this process. For EPP, on the other hand, the general trend of increasing thermal conductivity with longer aging can be observed, even though the beads are inhomogeneous in their morphology. The thermal conductivity increases over the aging time and at higher aging temperatures and can no longer be measured after 750 h at 140 °C. This investigation confirms the sensitivity of EPP to aging and higher temperatures. EPC on the other hand, exhibits
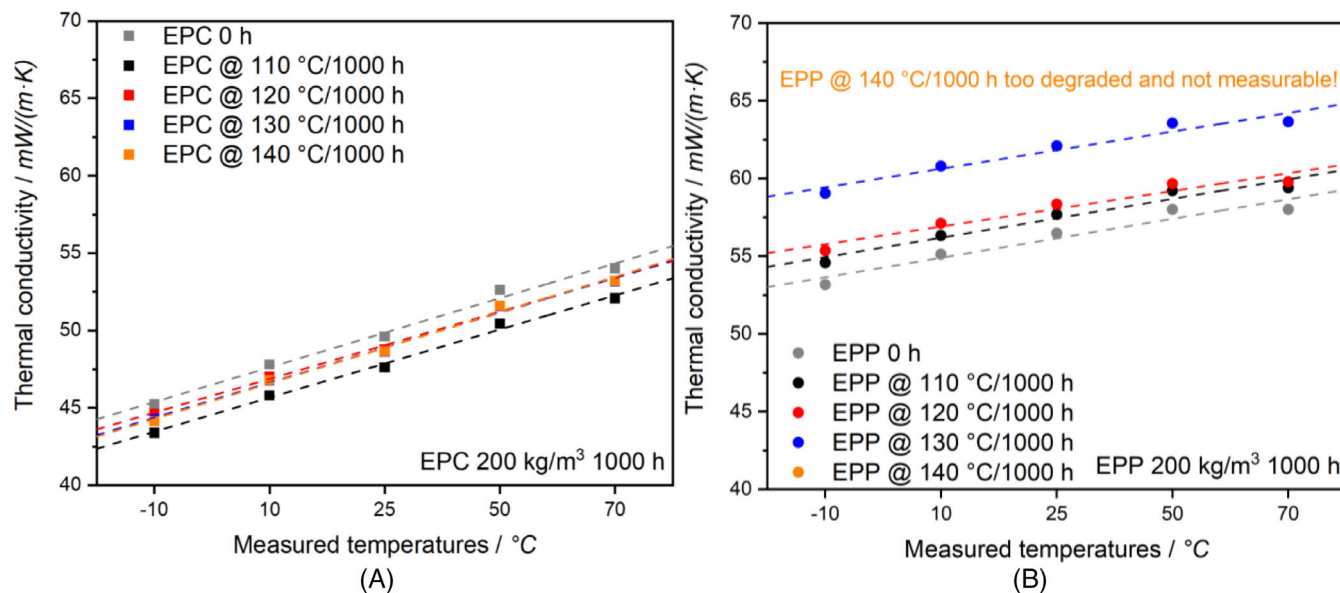
FIGURE 13   Temperature-dependent thermal conductivity of aged EPC and EPP for 1000 h at 110–140 °C.
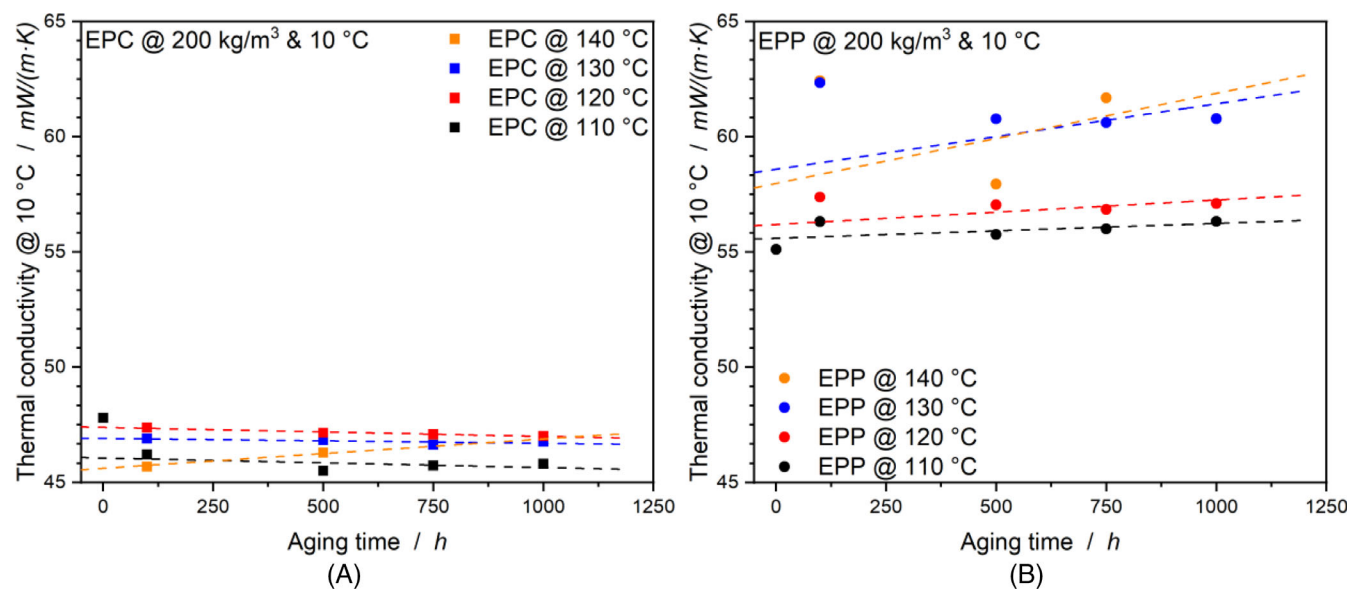

FIGURE 14   Influence of thermal aging on the thermal conductivity at 10 °C of EPC and EPP aged for 100–1000 h at 110–140 °C.

almost constant values over the whole range of aging experiments and can be concluded as a far more suitable material for temperature-challenging insulating applications. The complete dataset can be found in Table 7 of Data S1.

5 | CONCLUSION

To extend the range of application of bead foams to higher temperatures, new matrix materials such as expanded polycarbonate foam (EPC) have gained industrial interest due to their good thermo-mechanical properties. However, thermo-oxidative aging becomes significant when

thermoplastic foams are used at elevated temperatures. This aspect has received limited attention for bead foams thus far. Therefore, the objective of this work was to provide an overview of the effects of thermos-oxidative aging on properties relevant to foam applications, focusing on the mechanical and morphological properties of aged EPC and expanded polypropylene (EPP) as a reference.

Morphologically, EPC exhibits a slight increase in cell size under thermal-oxidative stress, accompanied by a minor decrease in density. EPP on the other hand, shows greater morphological stability. However, the crystallinity of EPP changes with aging time: it decreases at lower aging temperatures and increases over time at higher

aging temperatures. Additionally, OOT measurements in a differential scanning calorimeter (DSC) reveal an earlier onset of oxidation and a lower activation energy of oxidation for EPP compared with EPC.

Regarding mechanical properties, EPC displays less sensitivity to aging compared to EPP. Consequently, EPC-based bead foams exhibit significantly better compression properties after the same aging period when compared to EPP. The deterioration in compression properties of EPP is primarily attributed to pronounced embrittlement under thermal-oxidative stress. Interestingly, different aging behavior is observed in three-point bending: EPC shows constant modulus and strength over the aging period, with only a reduction in elongation at the maximum force before failure. This can be attributed to a deterioration in inter-bead interfacial strength due to aging. In contrast, EPP exhibits increasing modulus, strength and extensibility, potentially caused by thermally induced crystal rearrangement and post-crystallization within the bead-bead interface. Similar trends are observed in impact loading compared to three-point bending.

In terms of thermal conductivity, an initial decrease is observed for EPC, which correlates with its lower density. Conversely, EPP shows an increasing thermal conductivity with aging. However, no clear correlation with density, cell size or crystallinity is apparent. One possible reason for the increase in EPP's thermal conductivity might be the increasing open cell content.

ACKNOWLEDGMENTS

ORCID

Holger Ruckdäschel 🄳 https://orcid.org/0000-0001-5985-2628

ENDNOTE

[i] www.covestro.com/press/de/composites-fuer-den-wirtschaftlichen-leichtbau/.

REFERENCES

[1] E. Baur, T. A. Osswald, N. Rudolph, S. Brinkmann, E. Schmachtenberg, *Saechtling Kunststoff Taschenbuch*, 31st ed., Carl Hanser Verlag, München **2013**. https://doi.org/10.3139/9783446437296

[2] G. Ehrenstein, *Polymer Werkstoffe*, Carl Hanser Verlag GmbH & Co. KG, Munich **2011**, p. I. https://doi.org/10.3139/9783446429673.fm

[3] W. Kaiser, *Kunststoffchemie Für Ingenieure*, Carl Hanser Verlag GmbH & Co. KG, Munich **2015**, p. I. https://doi.org/10.3139/9783446447745.fm

[4] H. Bertilsson, B. Franzén, J. Kubát, *Makromol. Chem. Macromol. Symp.* **1990**, *38*, 115.

[5] T. W. Cheng, H. Keskkula, D. R. Paul, *J. Appl. Polym. Sci.* **1992**, *45*, 531.

[6] D. Dhara, A. Purushotham, N. Rosenquist, W. D. Richards, K. Maruvada, G. Chatterjee, *Polym. Eng. Sci.* **2009**, *49*, 1719.

[7] S. Suzuki, S. Nishitsuji, T. Inoue, *Polym. Eng. Sci.* **2012**, *52*, 1958.

[8] S. Redjala, R. Ferhoum, N. Aït Hocine, S. Azem, *J. Fail. Anal. Prev.* **2019**, *19*, 536.

[9] J. S. T. Steiner, G. Steiner, J. Koppelmann, T. H. Schwarz, *Die Angew. Makromol. Chemie*. **1988**, *158*, 321-334.

[10] I. Schwarz, M. Stranz, M. Bonnet, J. Petermann, *Colloid Polym. Sci.* **2001**, *279*, 506.

[11] M. Rjeb, A. Labzour, A. Rjeb, S. Sayouri, Y. Claire, A. Périchaud, *Phys. A: Stat. Mech. Appl* **2005**, *358*, 212.

[12] A. Law, L. Simon, P. Lee-Sullivan, *Polym. Eng. Sci.* **2008**, *48*, 627.

[13] A.-H. I. Mourad, *Mater. Des.* **2010**, *31*, 918.

[14] C. Delabroye, L. T. Nguyen, J.-F. Koenig, M. Heckmann, W. G. Stobby, C. P. Park, A. M. Chatterjee, Dimensionally-Stable Propylene Polymer Foam with Improved Thermal Aging. **2005**.

[15] P. C. Noble, B. Goode, T. A. Krouskop, B. Crisp, *J. Rehabil. Res. Dev.* **1984**, *21*, 31.

[16] M. B. Ramesh, S. R. Matu, S. T. Montgomery, S. B. Brijmohan, *J. Mater. Civ. Eng.* **2011**, *23*, 287.

[17] J. Smardzewski, Ł. Matwiej, *Drv. Ind.* **2013**, *64*(3), 201.

[18] N. Yarahmadi, A. Vega, I. Jakubowicz, *Polym. Degrad. Stab.* **2017**, *138*, 192.

[19] N. Weingart, D. Raps, J. Kuhnigk, A. Klein, V. Altstädt, *Polymers (Basel).* **2020**, *12*, 1.

[20] Z. Dobkowski, *Polimery/Polymers*. **2005**, *50*, 213.

[21] W. W. Focke, I. Van Der Westhuizen, *J. Therm. Anal. Calorim.* **2010**, *99*, 285.

[22] S. Ding, A. Khare, M. T. K. Ling, C. Sandford, L. Woo, *Thermochim. Acta* **2001**, *367*, 107.

[23] S. Wallius, *Die Angew. Makromol. Chemie*. **1993**, *212*, 103.

[24] C. L. De Carvalho, D. S. Rosa, *J. Therm. Anal. Calorim.* **2014**, *115*, 1627.

[25] D. Raps, Doctoral thesis, University of Bayreuth, (Bayreuth). **2020** https://doi.org/10.15495/EPub_UBT_00005200

SUPPORTING INFORMATION

Additional supporting information can be found online in the Supporting Information section at the end of this article.